

ARE TESSELLATED IMAGE OBJECTS REALLY RELIABLE?

I. Lizarazo ^{a*} and L. Araque ^b

^a Engineering Faculty, Universidad Distrital Francisco José de Caldas, Carrera 7 No. 40-53, Bogotá, Colombia

^b Centro de Investigación en Palma de Aceite, Calle 20 A N. 43A – 50, Bogotá, Colombia

ilizarazo[at]udistrital.edu.co,
laraque[at]cenipalma.org

KEY WORDS: image segmentation, object-oriented image analysis, image objects, vector to raster conversion

1. INTRODUCTION

Segmentation is the process of partitioning an image into multiple non-overlapping segments (image objects) (Blaschke *et al.*, 2006). Image segmentation is usually conducted using only data extracted from the input image (Freixenet *et al.*, 2002). The need for image segmentation is especially important in situations where real world objects are much bigger than pixels (Atkinson, 2004) and, additionally, landscape structure and geometry are unknown (Smith and Morton, 2010).

In many cases, image objects may be a more realistic representation of real world objects than individual pixels. However, in regions with high quality spatial information, where available GIS data sets provide accurate representations of real world objects, image segmentation should focus on matching image objects to existing vector objects rather than creating artificial image objects (Smith and Morton, 2010). A main problem with this “guided” image segmentation is that, even with fine pixel sizes, a raster-based solution for conducting such a task may lead to producing image objects with saw-toothed edges which barely match real world objects boundaries. The question here is: are tessellated image objects really reliable?

The error introduced in converting existing vector data to raster cells is very well documented (see, for example, Clarke, 1985; Veregin, 1989; Congalton, 1997). However, to the author’s knowledge, there is no research related to the influence of this topic on image objects definition. The objective of this paper is to determine whether the metric and thematic values generated from raster-based image objects are significantly different from “true” values provided by existing vector data sets.

For such a purpose, a method of defining boundaries of image objects based on vector data is proposed. The new method uses a vector square grid for pixel representation. Starting at a given pixel size, squares at boundaries are divided into smaller pieces to create realistic image objects boundaries which better reproduce the shape and appearance of real world objects. The proposed approach was applied to extract geometric and biophysical properties of agricultural plots from remotely sensed imagery. Vector-based and raster-based values were compared using paired t-tests which determined the level of statistical significance of the differences.

2. METHODS

2.1 Study Sites and Data

The study area is an oil palm plantation in Puerto Wilches (Colombia). The plantation encompasses 30 crop plots which cover approximately 224 ha. The terrain is flat with elevation 200 m ASL. Crop plots include different oil palm crop materials and ages. A Landsat TM image, acquired by NASA on February 2007, with pixel size of 30 m, was used in this experiment. For the study area, a vector polygon dataset derived through GPS survey is an accurate representation of crop plots boundaries. Figure 1 shows the vector crop plots, in blue color, overlaid over a RGB 745 color composition of the Landsat image.

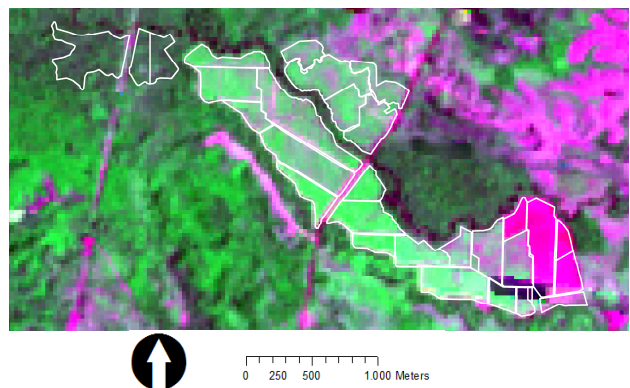


Fig. 1: Existing vector dataset of crop plots, outlined in white, overlaid over a RGB745 color composition of the Landsat-TM image.

2.2 Calculation of Vegetation Index

After doing an image-based atmospheric correction (Chavez, 1996), the Landsat image was used to obtain the normalized difference vegetation index (NDVI). The NDVI is a spectral variable that can be used as proxy data for crop health and photosynthetic capacity (Rouse *et al.*, 1974). The NDVI was computed by calculating the ratio of the VI (vegetation index, i.e., the difference between TM channels 4 and 3) and the sum of channels 4 and 3.

* corresponding author

2.3 Image-objects definition

The polygon data set representing crop plots was used as ground reference. Three of the polygons comprising this data set are shown in Figure 2. Note that this is clearly a high spatial resolution situation where pixels are much smaller than objects under study. Image objects were defined from the existing data set using a simple polygon to raster conversion procedure. The method used to determine how the cell will be assigned a value when more than one feature falls within a cell is the maximum area. In this method, the single feature with the largest area within the cell yields the attribute to assign to the cell. Cell size was defined as 30 m.

As shown in Figure 3, image objects created using such an approach exhibit a saw-toothed geometry very different than the smooth boundaries of crop plots.

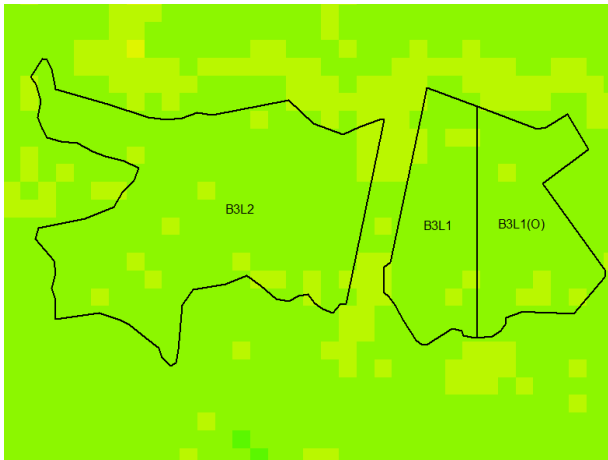


Fig. 2: Three polygons representing crop plots, outlined in black, overlaid over the NDVI image.

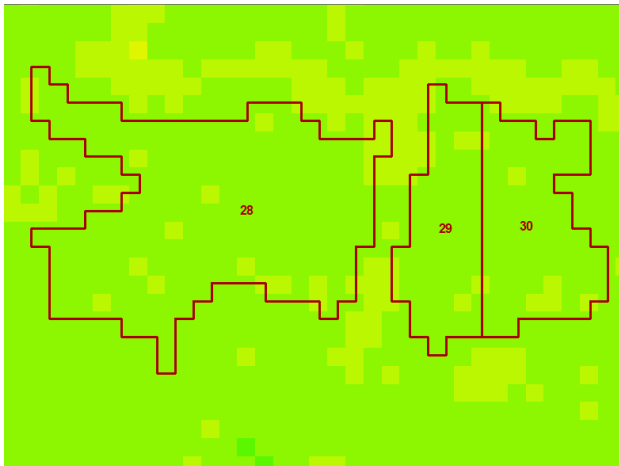


Fig. 3: Three raster-based image objects, outlined in red, overlaid over the NDVI image. Note the saw-toothed geometry.

Thus, a procedure to obtain *vector-based* image objects was conducted using three steps:

- (i) Pixels were vectorized and converted into square polygons;
- (ii) The resulting square polygons were intersected with the existing polygon data to divide boundary pixels into small pieces which replicate the outline of crop plots; and

- (iii) The output pieces were dissolved using the corresponding lot identifier as common attribute in order to group them into vector “image objects”.

The resulting image objects, shown in Figure 4, are composed of squares and smaller pieces which better replicate the true geometry of crop plots.

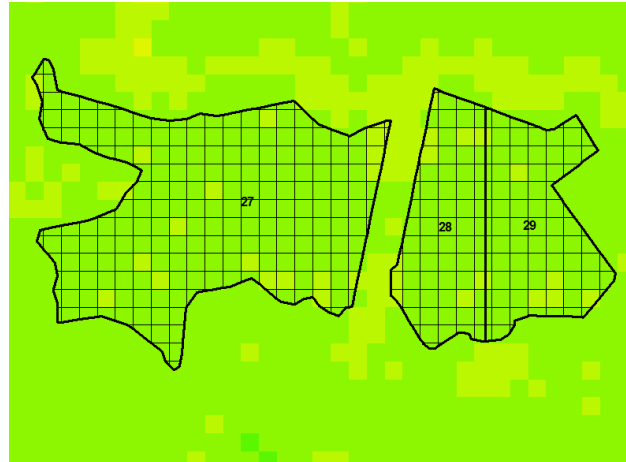


Fig. 4: Three vector-based image objects. Note that there is a one-to-one correspondence between image objects and crop plots. Each image object is composed of square pieces at core and smaller irregular pieces at boundaries.

2.4 Properties extraction

The resulting vector-based image objects were used to obtain geometric and biophysical properties for each plot. Area of each plot was calculated using equation (2):

$$A_p = a_1 + a_2 + \dots + a_n \quad (1)$$

where A_p is the plot's area, and a_n is the area occupied by piece n .

In addition, a weighted NDVI for each plot was calculated according to equation (1):

$$NDVI_p = a_1 * NDVI_1 + a_2 * NDVI_2 + \dots + a_n * NDVI_n \quad (1)$$

where $NDVI_p$ is the plot's NDVI, a_n is the area percentage occupied by piece n , $NDVI_n$ is the NDVI value at the pixel where the n piece is located, and $*$ is the product operator.

Once each image object has received its corresponding weighted NDVI value, a meaningful digital object has been created which resembles accurately both geometric and biophysical properties of its corresponding crop plot.

For comparison, the NDVI and area values of the conventional raster-based image objects were also computed. In such a case, area of each image object was calculated by counting its pixels and multiplying by the area of each pixel. Similarly, NDVI of each image object was calculated by a simple average of NDVI values for pixels comprising the object.

Comparison of area and NDVI values for vector-based and raster-based image objects was conducted using a paired t-test. The paired t-test null hypothesis was that the mean difference between the values obtained from the two methods was 0.

In order to examine sensitivity of raster-based area and NDVI values to cell's size, an additional test was conducted. In this case, conversion of existing polygons to image objects was done using coarser cell sizes, i.e. 60, 90 and 120 m. For each cell size, a bilinear convolution resampling technique was used to interpolate new pixel values for the Landsat image.

3. RESULTS AND DISCUSSION

Raster-based image objects (cell size of 30 m) and vector-based image objects provided similar results for the area and the NDVI values. In the paired t-test, no significant difference was found between the two methods. Table 1 shows results for area values. Table 2 shows results for NDVI values.

Table 1: Statistical results of the paired t-test for raster-based vs vector-based Area values (raster cell size of 30 m).

	<i>Vector</i>	<i>Raster</i>
Mean	7,471	7,452
Variance	20,907	21,217
Observations	30,000	30,000
Pearson Correlation	0,997	
Hypothesized Mean Difference	0,000	
df	29,000	
t Stat	0,293	
P(T<=t) one- tail	0,386	
t Critical one-tail	1,699	
P(T<=t) two-tail	0,771	
t Critical two-tail	2,045	

Table 2: Statistical results of the paired t-test for raster-based vs vector-based NDVI values (raster cell size of 30 m).

	<i>Vector</i>	<i>Raster</i>
Mean	0,159	0,156
Variance	0,014	0,015
Observations	30,000	30,000
Pearson Correlation	0,997	
Hypothesized Mean Difference	0,000	
df	29,000	
t Stat	1,288	
P(T<=t) one- tail	0,104	
t Critical one-tail	1,699	
P(T<=t) two-tail	0,208	
t Critical two-tail	2,045	

These results support the claim that when the analysis unit is significantly larger than cell size the “edge effect” of raster polygon boundaries is very low (Wade *et al.*, 2003).

Both the area and NDVI paired t-tests showed significant differences between vector and raster based image objects for coarse cell sizes, i.e. 60, 90 and 120 m. Figure 5 summarizes statistical results.

Table 4: Summary of statistical results of the paired t-test for raster-based vs. vector-based values.

	<i>Pixel size (m)</i>		
	60	90	120
Area values - t Stat	3,231	5,344	9,125
NDVI values - t Stat	2,833	3,201	5,644

In the conversion of polygon data sets to raster image objects, boundaries were distorted. Figures 5, 6, 7 and 8 show how raster cell size impacts geometry.

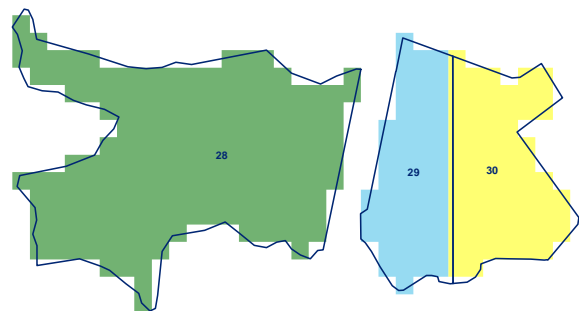


Fig. 5: Raster-based image objects, cell size 30 m, displayed under vector-based image objects.

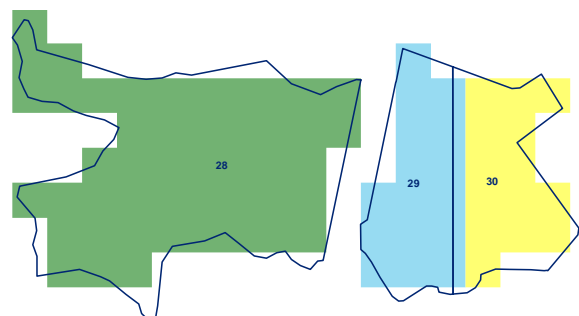


Fig. 6: Raster-based image objects, cell size 60 m, displayed under vector-based image objects.

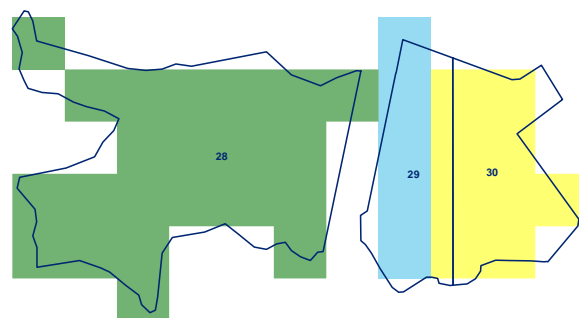


Fig. 7: Raster-based image objects, cell size 90 m, displayed under vector-based image objects.

According to results, cell size is a very important parameter to take into account when using image objects for analysis of both geometric and biophysical properties of real world objects.

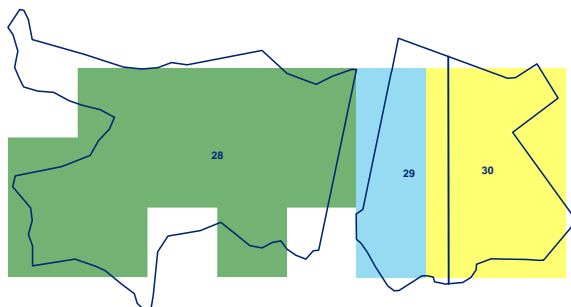


Fig. 8: Raster-based image objects, cell size 120 m, displayed under vector-based image objects.

It can be seen that when cell size approaches target object sizes, using raster-based image objects can lead to significant inaccuracies. In such cases, it could be advantageous to use vector-based image objects as those proposed in this paper.

4. CONCLUSIONS AND OUTLOOK

The purpose of this study was to learn how well geometric and biophysical properties of tessellated image objects represent “true” values. Raster-based and vector-based image objects were used to extract area and NDVI values for crop lots. It was shown that there may be significant differences in such values depending on raster cell size.

Atkinson (2001) raised a concern that remote sensing practitioners tended to choose images without properly considering if pixel size was appropriate for the study being conducted. The same could be said for object-based image analysis. GEOBIA users should make sure their analysis meet an H-resolution condition (i.e. pixel size is smaller than objects of interest) (Blasckhe *et al.*, 2006).

There is no a rule of thumb to define precisely when cell size is appropriate or not to create raster-based image objects. Much more research needs to be conducted to reach definitive answers. However, it could be suggested that a complete match of image objects to real-world objects is a must for a thorough integration between GEOBIA outputs and GIS processing tasks. It has been shown that, in many cases, accuracy of geometric properties impact greatly on accuracy of biophysical properties. This fact suggests the need to incorporate refined boundary data in GEOBIA studies.

The contribution of this paper can be summarized as follows:

- (1) A GIS-based method to refine image-objects geometry using existing vector data has been proposed.
- (2) The new method converts image primitives from the raster domain into the vector domain and adjust the resulting geometry to break real world objects into small pieces which better represent boundaries of real-world objects.
- (3) Experimental results demonstrate that the new method allows capturing differences on biophysical properties which are sometimes ignored using raster image objects which artificially tessellate the geographic space.

The proposed method can be used to optimize the conventional GEOBIA procedures which usually do not pay too much attention to create image objects with smooth boundaries. By doing that, it is expected that remote sensing products can be better integrated with existing GIS vector products. In addition, this study case suggests that, in many cases, image analysis would benefit of focusing much more on vector based object geometries than on tessellated geometries.

Acknowledgement

The Centro de Investigación en Palma de Aceite (CENIPALMA) provided the authors with the GIS vector datasets used in this research. The Landsat image was obtained from the Land Processes Distributed Active Archive Center (LP DAAC), located at USGS/EROS, Sioux Falls, SD. <http://lpdaac.usgs.gov>.

References

- Atkinson, P.M., 2001. Geostatistical Regularization in Remote Sensing. 237-260 in N. Tate, & P. Atkinson (Ed.), *Modelling Scale in Geographical Information Science*. Chichester: John Wiley & Sons Ltd.
- Atkinson, P.M., 2004. Spatially weighted supervised classification for remote sensing, *International Journal of Applied Earth Observation and Geoinformation*, 5, 277-291.
- Blasckhe, T., Burnett, C., Pekkarinen, A., 2006. Image segmentation methods for object-based analysis and classification. In S. de Jong & F. van der Meer, eds., *Remote Sensing Image Analysis: Including the Spatial Domain*, 211-236, Springer.
- Benediktsson, J.A., Pesaresi, M., Amason, K., 2003. Classification and feature extraction for remote sensing images from urban areas based on morphological transformations. *Geoscience and Remote Sensing, IEEE Transactions on*, 41(9), 1940-1949.
- Castilla, G., Hay, G.J., 2008. Image objects and geographic objects. In *Object-based Image Analysis*, 91-110. Springer.
- Chavez, P.S., 1996. Image based atmospheric corrections — Revisited and improved, *Photogrammetric Engineering and Remote Sensing*, 62:1025-1036.
- Clarke, K.C., 1985. A comparative analysis of polygon to raster interpolation methods. *Photogrammetric Engineering & Remote Sensing*, 51(5), 575-582.
- Congalton, R.G., 1997. Exploring and evaluating the consequences of vector-to-raster and raster-to-vector conversion, *Photogrammetric Engineering & Remote Sensing*, 63(4), 425-434.
- Freixenet, J., Muñoz, X., Raba, D., Martí, J. Cufí, X., 2002. Yet another survey on image segmentation: Region and boundary information integration. *Lecture Notes in Computer Science*, 2352, 408-422.
- Rouse, J.W. Jr., R.H. Haas, D.W. Deering, J.A. Schell, and J.C. Harlan, 1974. *Monitoring the Vernal Advancement and Retrogradation (Green Wave Effect) of Natural Vegetation, Greenbelt: NASA/GSFC Type III Final Report*, 371 pp.
- Smith, G.M., Morton, R.D., 2010. Real World Objects in GEOBIA through the Exploitation of Existing Digital Cartography and Image Segmentation. *Photogrammetric Engineering & Remote Sensing*, 76(2), 163-171.
- Veregin, H., 1989. A review of error models for vector to raster conversion, *The Operational Geographer*, 7(1):11-15.
- Wade T.G., Wickham, J.D., Nash M.S., Neale A.C., Riitters K.H., Jones K.B., 2003. A Comparison of Vector and Raster GIS Methods for Calculating Landscape Metrics Used in Environmental Assessments. *Photogrammetric Engineering & Remote Sensing*, 69(12), 1399-1405.